Available online at www.sciencedirect.com
SCIENCE DIRECT®
Journal of Nuclear Materials 322 (2003) 152–164
journal of nuclear materials
www.elsevier.com/locate/jnucmat

Chemically durable iron phosphate glasses for vitrifying sodium bearing waste (SBW) using conventional and cold crucible induction melting (CCIM) techniques

C.W. Kim [a,*], C.S. Ray [a], D. Zhu [a], D.E. Day [a], D. Gombert [b], A. Aloy [c], A. Moguš-Milanković [d], M. Karabulut [e]

[a] *Graduate Center for Materials Research, University of Missouri-Rolla, 101 Straumanis Hall, Rolla, MO 65409-1170, USA*
[b] *Idaho National Engineering and Environmental Laboratory, Idaho Falls, ID 83415, USA*
[c] *V.G. Khlopin Radium Institute, St. Petersburg, Russia*
[d] *Department of Physics, Ruđer Bošković Institute, Bijenička c.54, 10000 Zagreb, Croatia*
[e] *Department of Physics, University of Kafkas, 36000 Kars, Turkey*

Received 26 November 2002; accepted 26 June 2003

Abstract

A simulated sodium bearing waste (SBW) was successfully vitrified in iron phosphate glasses (IPG) at a maximum waste loading of 40 wt% using conventional and cold crucible induction melting (CCIM) techniques. No sulfate segregation or crystalline phases were detectable in the IPG when examined by SEM and XRD. The IPG wasteforms containing 40 wt% SBW satisfy current DOE requirements for aqueous chemical durability as evaluated from their bulk dissolution rate (D_R), product consistency test, and vapor hydration test. The fluid IPG wasteforms can be melted at a relatively low temperature (1000 °C) and for short times (<6 h). These properties combined with a significantly higher waste loading, and the feasibility of CCIM melting offer considerable savings in time, energy, and cost for vitrifying the SBW stored at the Idaho National Engineering and Environmental Laboratory in iron phosphate glasses.

PACS: 28.41.Kw; 60; 80

1. Introduction

Vitrification of nuclear waste in a suitable glass is considered the preferable process for waste disposal. The US Department of Energy (DOE) currently approves only borosilicate (BS) type glasses for such purposes. However, many high level nuclear waste (HLW), presently awaiting disposal, have complex and diverse chemical compositions, and often contain components such as phosphates, sulfates, chrome oxide, and heavy metals that are poorly soluble in BS glasses [1,2]. Such problematic wastes can be pre-processed and/or diluted to compensate for their incompatibility with a BS glass matrix, but this will typically increase the wasteform volume and the overall cost for vitrification. Direct vitrification using alternative glasses that use the major components already present in the waste is preferable, since it would avoid pre-treating or diluting the waste, and, thus, minimize the wasteform volume and overall cost.

The Idaho National Engineering and Environmental Laboratory (INEEL) stores approximately 5.7 million liters of sodium bearing waste (SBW) and plans for its disposal between 2007 and 2012 [2]. The SBW composition is relatively high in sodium, aluminum, and sulfate (see Table 1). The poor solubility (<1 wt%) of sulfate in the BS glasses limits the waste loading to a maximum of

* Corresponding author. Tel.: +1-573 341 4359; fax: +1-573 341 2071.
E-mail address: cheol@umr.edu (C.W. Kim).

0022-3115/$ - see front matter © 2003 Elsevier B.V. All rights reserved.
doi:10.1016/S0022-3115(03)00325-8

Table 1
Nominal composition and raw materials used to prepare INEEL simulated SBW

Oxide	wt%
Na_2O	52.3
Al_2O_3	27.8
K_2O	7.6
CaO	2.2
Fe_2O_3	1.4
MnO	0.8
P_2O_5	1.6
B_2O_3	0.4
MgO	0.4
Cr_2O_3	0.2
SO_3	3.6
Cl	0.9
F	0.8
Total	100.0
Raw material	
$NaNO_3$	68.3
Al_2O_3	14.4
KNO_3	8.4
CaO	0.6
Fe_2O_3	0.7
MnO	0.4
$NaPO_3 \cdot 3H_2O$	1.8
H_3BO_3	0.3
MgO	0.2
Cr_2O_3	0.1
Na_2SO_4	3.3
NaCl	0.7
CaF_2	0.8
Total	100.0

only 20 wt% [3], which would result in an increased cost and a high wasteform volume. These are possibly the reasons that the plans for disposing of the SBW using vitrification process have been discontinued at INEEL. However, our present work demonstrates that vitrification of the SBW in iron phosphate glasses could substantially reduce the cost and wasteform volume and, therefore, may be considered as a viable option.

The main objective of the present study was to investigate the feasibility of using iron phosphate glasses (IPG) to vitrify the SBW at INEEL with an aim of producing a wasteform of the highest possible waste loading combined with acceptable chemical durability. Melting these IPGs in a cold crucible induction melter (CCIM) has also been explored in a preliminary fashion, since this technique eliminates many materials and operating constraints, such as the chemical corrosion of the melter refractories and metal electrodes, which is unavoidable in a joule-heated melter (JHM) such as that now being used to vitrify nuclear waste at the Savannah River Site.

2. Experimental

2.1. Preparation of simulated SBW

A supply of the simulated SBW was prepared using the raw materials listed in Table 1. The composition was simplified by neglecting components present in quantities less than 0.1 wt% in the original SBW. The slight difference in composition is not expected to affect the overall properties and test results.

The appropriate amounts of the raw materials were ground to pass through a 100 mesh sieve, dry mixed by tumbling in a sealed plastic container and then stored in a sealed container until used. With the raw materials listed in Table 1, the calculated weight loss on ignition for the SBW was 48.6% assuming all nitrates and water volatilized during melting. A detailed mass balance including feed, final glass, and volatiles is described in Section 3.2.

2.2. Preparation and melting of wasteforms in an electric furnace

The mixture of simulated SBW, along with the two additives Fe_2O_3 and P_2O_5, was thoroughly dry mixed and then melted in a high purity alumina crucible in an electric furnace. The amount of P_2O_5 used in the batch included an additional 5 wt% of the required amount in order to compensate for volatilization losses of P_2O_5 during melting. A total of 600 g of IPG containing 40 wt% of the SBW (denoted as IP40WG) was prepared by melting the batch at 1000 °C for 3 h. The melt was stirred at 1000 °C with an alumina rod at 30 min intervals to aid melt homogenization. Most of the melt was poured onto a steel plate and cooled quickly to room temperature without annealing. A small portion (a few grams) of the melt was also poured into steel molds to form rectangular bars, 1 cm × 1 cm × 5 cm, for dissolution rate measurements. These bars were annealed at 420 °C for approximately 4 h and slowly cooled overnight in the annealing furnace to room temperature.

2.3. Preparation and melting of wasteforms in a cold crucible induction melter

A batch whose glass composition is the same as that of the IP40WG was prepared by mixing appropriate amounts of individual raw materials instead of mixing additives in the simulated SBW as was done for melting in an electric furnace (Section 2.2). The raw materials included $Al(PO_3)_3$, Na_2CO_3, K_2CO_3, CaO, Fe_2O_3, H_2SO_4, and H_3PO_4. An appropriate amount (18 g) of a sacrificial conductive material (silicon carbide in this case) to initiate the melting process was thoroughly mixed with the batch. A total of 1007 g of the batch was fed into the cold crucible, fabricated from stainless steel,

inside a copper inductor in a shield box. The batch was melted for 1 h in a high frequency field (1.76 MHz) at a power level of 10–30 kW depending upon the stage of melting. The melting temperature was not measured. The gases formed during the melting process were evacuated from the shield box through an aerosol filter to a special ventilation system. After melting, 797 g of IPG (denoted as IP40WG-CCIM) out of 1007 g batch was obtained, indicating a 21% weight loss due to volatile components (see Section 3.2). This was the first experimental melting of an IPG wasteform in a CCIM and was conducted at the V.G. Khlopin Radium Institute in St. Petersburg, Russia. A detailed description of the CCIM technique is given in [3].

2.4. General property measurements

The density of each glass (IP40WG and IP40WG-CCIM) was measured at room temperature by the Archimedes' method using deionized water (DIW) as the suspending medium. The estimated error was ±0.01 g/cm^3. The glass transition (T_g) and crystallization (T_x) temperatures were measured by differential thermal analysis (DTA-7, Perkin Elmer) in flowing nitrogen at a heating rate of 10 °C/min. The estimated error was ±3 °C for T_g and T_x. Mass balance including feed (batch), final glass, and volatiles was measured for melting in both an electric furnace and CCIM.

The liquidus temperature (T_l) was measured per ASTM C 829-81 procedures in a temperature gradient furnace using a platinum tray in which glass particles were fused to form a thin (~3 mm) layer of melt. The platinum tray holding the melt remained in the furnace for 24 h to ensure that equilibrium between the crystal and glassy phases was established. The liquidus temperature of each glass was measured twice and then averaged. Precision of the liquidus temperature between two independent measurements in the same furnace was ±5 °C.

2.5. High temperature viscosity

The viscosity of the two melts in their melting range (900–1200 °C) was measured using a Brookfield rotating viscometer modified for high temperature use. A non-standard alumina spindle was made from a 10 cc straight wall crucible. Three standard viscosity oils (97.2, 98.8, and 965 centipoise) were used to calibrate the viscosity device. Repeated measurements indicated that the estimated error was <±5%. Each melt was thermally equilibrated at a selected temperature for 30 min, whereupon, a pre-heated spindle (located just above the melt) was immersed in the melt. Spindle speeds of 10, 20, and 50 rpm were used for each measurement. The viscosity of each melt was measured three times (at each temperature and spindle speed) and then averaged.

2.6. High temperature ac electrical conductivity

The ac electrical conductivity for the melts was measured between 900 and 1300 °C at 120 Hz and 1 kHz. Two parallel Pt/10% Rh electrodes were immersed in the melt, the dimension of the immersed part of the electrodes was 1 cm × 2 cm. The distance between the two electrodes was 1.5 cm. The resistance between the two electrodes in the melt was measured directly by a LCR meter, and the resistance was converted to ac electrical conductivity (σ) using the equation:

$$\sigma = K\left(\frac{1}{R}\cdot\frac{L}{S}\right), \tag{1}$$

where R is the measured electrical resistance, L the distance between the two electrodes, S is the surface area of the electrode immersed in the melt, and K is the cell constant that was determined by calibrating the instrument using three different concentrations of KCl standard solution [4]. The estimated error was ±5% or less.

2.7. Chemical durability

The chemical durability for the IP40WG and IP40WG-CCIM glasses was measured by three different methods: (1) dissolution rate (D_R) calculated from the weight loss of bulk samples immersed in DIW at 90 °C [5], (2) product consistency test (PCT) [6], and (3) vapor hydration test (VHT) [7]. The last two methods, namely, PCT and VHT, are recommended by DOE for determining the chemical durability, although our previous measurements [5] show that the D_R values are always in good agreement with the PCT and VHT results.

2.7.1. Dissolution rate (D_R)

Specimens were diamond sawed (using kerosene for cooling) from the annealed glass bars and then ground progressively using 240, 600, and 800 grit SiC papers. The dimensions of each specimen were measured (±0.002 cm) and were approximately 1 cm × 1 cm × 1 cm. The specimens were rinsed with acetone and DIW, dried at 90 °C, cooled to room temperature, and then weighed (±0.01 mg). Each specimen was suspended by a thin rayon thread in a Pyrex™ flask containing 100 ml of DIW. The flasks containing the specimens were placed in an oven at 90 ± 2 °C. Specimens were removed after 8, 16, or 32 days, rinsed with DIW, dried at 90 °C, cooled, and weighed (±0.01 mg).

The dissolution rate (D_R) was calculated from the measured weight loss (ΔW) using the equation:

$$D_R = \frac{\Delta W\ (\mathrm{g})}{A\ (\mathrm{cm}^2)\times t\ (\mathrm{min})}, \tag{2}$$

where A is the surface area (cm^2) of the specimen and t is the time (min) that the specimen was immersed in the

test solution at 90 °C. The weight loss (ΔW) is $W_i - W_t$, where W_i is the initial weight and W_t is the weight of the same specimen after a time t in DIW at 90 °C.

All tests were carried out in triplicate and the values averaged. The pH of the leachate was measured each time the sample was removed. Samples from a borosilicate environmental assessment (EA) glass provided by the defense waste processing facility (DWPF) at Westinghouse Savannah River Co. were also measured at the same conditions. The values of D_R for the EA glass were used as reference to evaluate the chemical durability of the iron phosphate glasses.

2.7.2. Product consistency test (PCT)

The PCT was conducted following the procedures described in ASTM C 1285–97 [6]. The glass powder (−100 to +200 mesh) was washed twice with flowing DIW and then ultrasonically washed twice with DIW to remove any small dust particles adhering to the surface of the larger particles. Finally, the sample was ultrasonically washed twice with ethanol to dissolve any organic materials, and dried at 90 °C overnight. Exactly 1.5 g of glass powder (±0.01 mg) was mixed with 15 ml of DIW in a Teflon vessel held at 90 ± 2 °C for seven days. After completion of the PCT, the leachate was filtered using a Nalgene 0.45 μm syringe filter and the concentration of ions in the leachate was measured by inductively coupled plasma-emission spectroscopy (ICP-ES). Leachate losses were less than 1% of the initial volume of leachant during the test. All tests, including pH measurements, were conducted in duplicate and the results averaged.

The normalized elemental mass release, r_i, was calculated from Eq. (3):

$$r_i\ (\mathrm{g/m^2}) = \frac{C_i}{f_i(A/V)}, \tag{3}$$

where C_i is the concentration of element i in the leachate ($\mathrm{g/m^3} = \mathrm{ppm} = \mu\mathrm{g/ml} = \mathrm{mg/l}$) and f_i is the mass fraction of element i in the glass (unitless), which was calculated using the analyzed glass composition given in Table 2. A/V is the ratio of the sample surface area to volume of leachate ($\mathrm{m^{-1}}$). A value of 1953 $\mathrm{m^{-1}}$ for A/V as calculated per the procedures in ASTM C 1285–97 [6] was used for both samples (IP40WG and IP40WG-CCIM).

2.7.3. Vapor hydration test (VHT)

Specimens were cut from rectangular glass bars with a diamond saw and all sides were polished to 600 grit SiC paper. The specimens ($\sim 10 \times \sim 10 \times \sim 1.5\ \mathrm{mm^3}$) were rinsed successively with acetone and DIW, after which the dimensions and weight were measured to an accuracy of ±0.002 mm and ±0.01 mg, respectively. Two specimens from each glass were suspended by a Teflon thread connected to a stainless steel support. The support along with the specimens was placed inside a Parr 22 ml T304 stainless steel vessel together with 0.25 ml of DIW. The sealed vessel containing the sample was heated at 200 ± 2 °C in an automated temperature-controlled oven for 7 days. After removing the sample from the vessel, the sample was cross-sectioned and polished. The cross-section of each sample was examined and the thickness of the uncorroded part of the sample was measured with an accuracy of ±0.002 mm by an optical microscope. For a more detailed description of the VHT procedures, see [7].

Table 2
Batch and analyzed (ICP-ES) compositions (wt%) of iron phosphate glasses containing 40 wt% SBW

Oxide (wt%)	IP40 WG		IP40WG-CCIM	
	Batch	ICP-ES	Batch	ICP-ES
Na_2O	20.5	23.2	21.9	19.4
Al_2O_3	10.9	12.7	11.6	13.0
K_2O	3.0	3.2	3.2	4.4
CaO	0.9	0.8	0.9	0.7
Fe_2O_3	10.3	11.5	10.6	10.9
MnO	0.3	0.4	NP	0.0
P_2O_5	51.7	47.3	50.0	48.5
B_2O_3	0.1	NM	NP	NM
MgO	0.2	0.1	NP	0.0
Cr_2O_3	0.1	0.1	NP	0.0
SO_3	1.4	0.6[a]	1.8	0.0[a]
Cl	0.3	NM	NP	NM
F	0.3	NM	NP	NM
SiO_2	NP	NP	NP	3.4
Total	100.0	99.9	100.0	100.3

IP40WG and IP40WG-CCIM were melted in an electric furnace and in the cold crucible induction melter, respectively.
NM = not measured.
NP = not present.
[a] Analyzed by Leco.

The corrosion rate, m_d/t ($\mathrm{g/m^2/day}$), of the specimen was calculated from the dissolved mass of the specimen (Δm); the difference between the initial thickness (d_i) and the thickness of the remaining (uncorroded) part (d_r) of the same specimen, the specimen surface are (A), and the duration of test, t (7 days) using the equation:

$$m_d/t = \frac{\Delta m}{A \cdot t} = \frac{m_i - m_r}{2(w_i l_i + l_i d_i + d_i w_i) \cdot t} \approx \frac{\rho w_i l_i d_i - \rho w_i l_i d_r}{2 w_i l_i \cdot t} = \frac{\rho(d_i - d_r)}{2 \cdot t}, \tag{4}$$

where m_i is the initial weight and m_r is the weight of the uncorroded part of the same specimen, ρ is the specimen density, w_i is the initial width and l_i is the initial length of the specimen.

2.8. Analytical methods

The chemical composition of each glass was measured by ICP-ES and by Leco for sulfur analysis. ICP-ES was also used to measure the concentration of ions in the leachate after completion of the PCT. All of the ICP-ES and Leco analyses in this study were conducted by Acme Analytical Laboratories Ltd. in Vancouver, Canada.

The pH of the test solutions from D_R, PCT, and VHT was measured by a FisherScientific Accumet® pH/ion meter (model 25) with an accuracy of ±0.02 pH units. A three point pH calibration for the meter was performed with buffer solutions of pH 4.00, 7.00, and 10.00 before each measurement.

Optical microscopy (OM) and JEOL T330A scanning electron microscopy (SEM) operated at 15–20 kV were used to examine the chemical homogeneity of the IPGs. OM and SEM were also used to observe the appearance of glass samples after performing the D_R, PCT, and VHT chemical durability tests.

A Scintag PADX X-ray diffractometer (XRD), which uses CuK_α radiation with a wavelength of 1.5418 Å, was used to examine glass homogeneity and identify any crystalline phases in samples after VHT.

The valence state of iron ions (Fe(II) and Fe(III)) and their concentration in the glasses were measured by Mössbauer spectroscopy using 200 mesh powdered glass samples. Mössbauer spectra were obtained at room temperature on a constant acceleration spectrometer (ASA600) that utilized a 50 mCi rhodium matrix cobalt-57 source. The spectrometer was calibrated at room temperature with an α-iron foil and the line width of the α-iron spectrum was 0.27 mm/s. Each spectrum was fitted with eight broadened paramagnetic Lorentzian doublets. Details of this fitting procedure are given elsewhere [8].

The IR spectra of glasses were measured from 400 to 1600 cm^{-1} with a reflectance setup using a Fourier transform infrared (FT-IR) spectrometer (Nicolet Magna 750). The samples for FT-IR were cut from rectangular glass bars ($\sim 10 \times \sim 10 \times \sim 2$ mm^3) and polished to 1200 grit SiC paper. The spectrometer was purged with filtered dry air. Thirty two scans were collected for each sample and averaged.

Raman spectra were obtained using 200 mW of 514.5 nm light from an Innova 100 coherent argon-ion laser and were recorded by a computerized triple monochromator Dilor model Z 24 at Ruđer Bošković Institute, Croatia. A 90° scattering geometry was used with the sample oriented at a near-grazing angle. The complex shape of the experimentally recorded Raman bands was analyzed using a least-squares fitting procedure and assuming a Gaussian shape. Typically about 100 iterative steps were performed to obtain a good fit.

3. Results and discussion

3.1. Glass formation

The chemical composition of each glass melted in either a refractory crucible in an electric furnace or the cold crucible induction melter (IP40WG and IP40WG-CCIM, respectively) was calculated from the batch composition and measured by ICP-ES and Leco (Table 2). The calculated and analyzed compositions were in satisfactory agreement with each other. The chemical composition for the wasteform melted in the CCIM was close to that for the wasteform prepared in the electric furnace, but contained about 3.4 wt% SiO_2. The source of this SiO_2 was the silicon carbide that was added to the batch as a sacrificial conductive material (susceptor) to initiate the melting process in the CCIM.

The molar ratio of oxygen to phosphorus (O/P) calculated from the batch as well as measured compositions was 3.9, for both IP40WG and IP40WG-CCIM glasses. This value is slightly higher than the previously reported [5] range of O/P values, from 3.4 to 3.7, that yield the best glass forming tendency and chemical durability.

SEM and powder XRD did not reveal any sulfate segregation, inclusions, nodules, or crystalline phases in either sample, IP40WG and IP40WG-CCIM, suggesting that both glasses were chemically homogeneous. There was no observable sulfate 'gall' layer on the surface of the molten IPG, as has been reported [9] for borosilicate melts that contained >1 wt% SO_3. Leco analysis indicated that about 43 wt% of the sulfate originally present in the waste was retained in the IP40WG (Table 2). However, no sulfate was detected by Leco analysis in the IP40WG-CCIM, implying that most of the sulfate apparently volatilized as SO_2 during the melting in the CCIM. This volatilization could be explained by the more reducing conditions (verified by Mössbauer spectra, discussed later) in the CCIM melt because of the significant amounts of redox sensitive chemicals, such as carbonates and the silicon carbide as raw materials and a susceptor, respectively. The temperature for the IP40WG-CCIM melt in the cold crucible induction melter was not measured, but is believed to be much higher than the 1000 °C used to melt IP40WG in the electric furnace. A higher melting temperature would also have increased the volatilization of the sulfate and made the melt more reducing [10,11].

3.2. General properties

Selected properties such as density, glass transition (T_g) temperature, crystallization (T_x) temperature, and liquidus (T_l) temperature for the IP40WG and IP40WG-CCIM samples are summarized in Table 3. The mass balance including feed, final glass, and volatiles was calculated using several assumptions and was measured

Table 3
General properties of IP40WG and IP40WG-CCIM waste-forms

Properties	IP40WG	IP40WG-CCIM
Glass density (g/cm^3)	2.76 ± 0.01	2.76 ± 0.01
T_g (°C)	430 ± 3	420 ± 3
T_x (°C)	590 ± 3	560 ± 3
T_l (°C)	740 ± 5	718 ± 5

T_g = glass transition temperature, T_x = crystallization temperature, and T_l = liquidus temperature.

for the glasses prepared under both melting conditions, electric furnace (IP40WG) and cold crucible induction melter (IP40WG-CCIM) (Table 4). The measured and calculated values are in good agreement.

3.3. High temperature viscosity

The viscosity (η) for the IP40WG and IP40WG-CCIM melts were measured from 900 to 1200 °C at three different spindle speeds, 10, 20, and 50 rpm. Since the values of η at any given temperature for three spindle speeds were very close to each other (<±5%), these values were averaged and reported in Fig. 1(a) as a function of temperature. The values of η for a baseline iron phosphate melt, $43Fe_2O_3 \cdot 57P_2O_5$, wt% (F43), are also included in Fig. 1(a) for comparison. The lower viscosity at any temperature for the two melts containing SBW compared to that for F43 is consistent with their higher soda content. The IP40WG-CCIM melt had a slightly higher viscosity than the IP40WG melt. This may be due to the presence of silica in the IP40WG-CCIM melt from the sacrificial conductive silicon carbide used to initiate the melting process in the CCIM.

The plot of log viscosity (η) vs. $1/T$ in Fig. 1(b) indicates that the viscosity obeyed the Arrhenius equation over the melting range. The activation energy (Q) for viscous flow was calculated from the slope of the curves in Fig. 1(b) and had the values 47.3, 67.0, and 108.0 kJ/mol for the IP40WG, IP40WG-CCIM, and baseline IPG (F43), respectively. These values of Q for the iron phosphate melts are considerably smaller than the reported [12] Q of 514.9 kJ/mol for the SiO_2 melt (1600–2500 °C) or of 173.7 kJ/mol for the P_2O_5 melt (545–655 °C).

Iron phosphate melts are 10–100 times more fluid than most silicate melts as indicated by the viscosity curves for the iron phosphate melts in Fig. 1. At their melting temperature (1000 °C), the viscosity is approximately 5–9 poise so a melting time of only a few hours is typically adequate to achieve a chemically homogeneous melt free of all batch materials.

Table 4
Calculated and measured mass balance including feed, final glass, and volatiles during the melting process in both electric furnace and cold crucible induction melter

Calculated assumptions	IP40WG			
	Batch (g)	Glass (g)	Volatiles (g)	Volatiles (%)
1. Lose NO_3 and H_2O	886.0	647.1	238.9	27.0
2. Lose NO_3, H_2O, and 5 wt% P_2O_5	886.0	630.6	255.4	28.8
3. Lose NO_3, H_2O, and SO_3	886.0	638.1	247.9	28.0
4. Lose NO_3, H_2O, SO_3, and 5 wt% P_2O_5	886.0	621.5	264.5	29.8
5. Lose NO_3, H_2O, and Cl	886.0	646.0	240.0	27.1
6. Lose NO_3, H_2O, Cl, and 5 wt% P_2O_5	886.0	629.4	256.6	29.0
7. Lose NO_3, H_2O, SO_3, and Cl	886.0	635.9	250.1	28.2
8. Lose NO_3, H_2O, SO_3, Cl, and 5 wt% P_2O_5	886.0	619.4	266.6	30.1
Measured during melting in electric furnace	886.0	625.1	260.9 ± 10	29.4 ± 1
	IP40WG-CCIM			
1. Lose CO_2 and H_2O	1007.0	851.8	155.2	15.4
2. Lose CO_2, SO_3, and H_2O	1007.0	835.7	171.3	17.0
Measured during melting in CCIM	1007.0	797.0	210.0 ± 10	20.9 ± 1

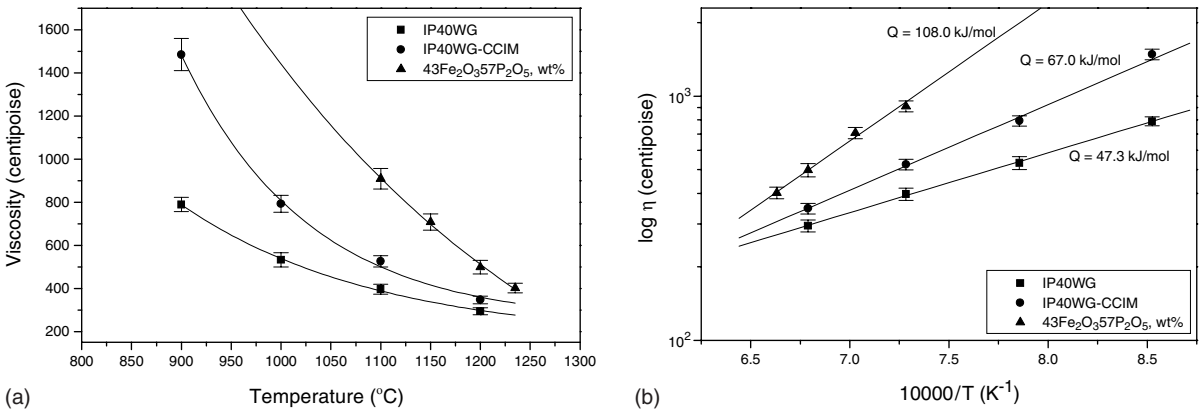

Fig. 1. Viscosity (η) of melts IP40WG and IP40WG-CCIM near their melting temperature range. Data for a $43Fe_2O_3 \cdot 57P_2O_5$ (wt%) glass is shown for comparison. (a) Viscosity (centipoise) vs. temperature (°C); (b) viscosity (centipoise-log scale) vs. temperature (K^{-1}). Activation energy (Q) for viscous flow was determined from the slope $\log \eta$ vs. $1/T$.

3.4. High temperature ac electrical conductivity

The ac electrical conductivity (σ) of the IP40WG and IP40WG-CCIM melts shown in Fig. 2 was essentially the same at any temperature from 900 to 1300 °C and followed an Arrhenius temperature dependence. The ac frequency had practically no effect on σ, at least in the range between 1 and 120 kHz used in the present investigation. The electrical conductivity increased from 40 S/m at 900 °C to 160 S/m at 1300 °C for both iron phosphate melts. This range of conductivity is 2–3 times higher than that of a borosilicate melt (SBW-22-20 [13]) which contains 20 wt% SBW. The higher electrical conductivity for IPG melts suggests that IPG wasteforms can be easily processed in the CCIM, as has been confirmed by the current experience of melting IP40WG-CCIM.

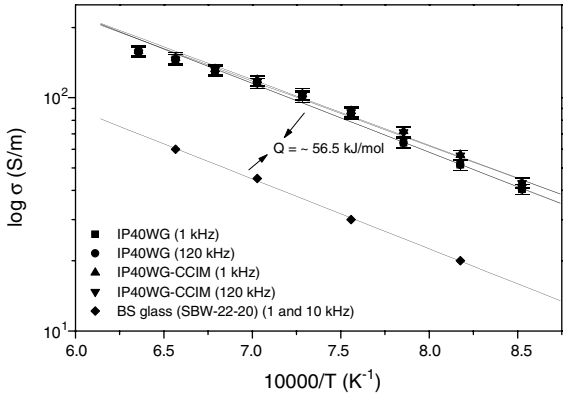

Fig. 2. Electrical conductivity (σ) of IP40WG and IP40WG-CCIM melts near their melting temperature range. For comparison, BS glass data (SBW-22-20: borosilicate glass wasteform containing 20 wt% SBW) provided by PNNL [13] is given. Activation energy (Q) for electrical conductivity was calculated from the slope $\log \sigma$ vs. $1/T$.

In alkali-containing iron phosphate glasses, the electrical conductivity generally consists of both electronic and ionic conduction [14,15]. However, recent studies [16,17] have shown that alkalis such as sodium and potassium ions have such a low mobility in alkali-containing iron phosphate glasses that they make no detectable contribution to the total conductivity. The electrical conduction in IP40WG and IP40WG-CCIM melts is believed to occur mainly by electrons hopping from Fe(II) to Fe(III) ions. The activation energy (Q) of 56.5 kJ/mol, determined from the slope of the curves in Fig. 2, for the IP40WG and IP40WG-CCIM melts is similar to the activation energy for dc conduction (53.1 kJ/mol) for other sodium-containing iron phosphate glasses [17], which have been identified as electronic conductors.

The borosilicate melt (SBW-22-20 [13]) has the same activation energy (56.5 kJ/mol) as that of the IPG melts (Fig. 2), suggesting that conduction in the BS melt may be due primarily to the multi-valence elements (electronic) such as vanadium and iron in the SBW-22-20 wasteform. However, the content of these elements is relatively small (4.0 wt% V_2O_5 and 1.5 wt% Fe_2O_3) in the SBW-22-20 borosilicate wasteform, which may be the reason for its overall lower conductivity than the IPG, as shown in Fig. 2.

3.5. Chemical durability

The D_R of the iron phosphate IP40WG and IP40WG-CCIM glasses and the borosilicate EA glass is shown in Fig. 3 as a function of time the samples were immersed in DIW. Also shown in Fig. 3 is the pH of the leachate after the end of each test, the initial pH of the leachant being 5.8. The D_R of the present IP40WG and

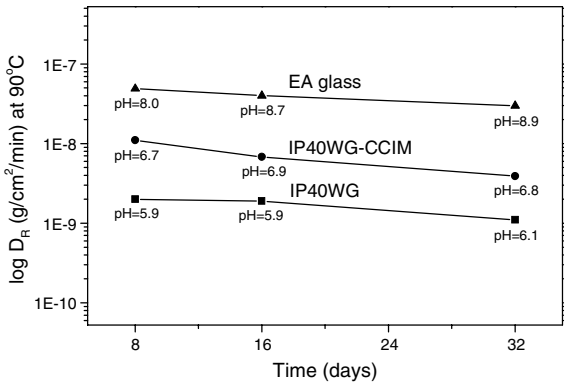

Fig. 3. Dissolution rate (D_R = g/cm^2/min) in DIW at 90 °C for iron phosphate glasses (IP40WG and IP40WG-CCIM) and EA glass (provided from DWPF). Initial pH of DIW was 5.8. Note the nearly constant pH of the leachate for the IP40WG and IP40WG-CCIM samples which is due to the larger buffering action (compared to silicate glasses) of phosphate glasses.

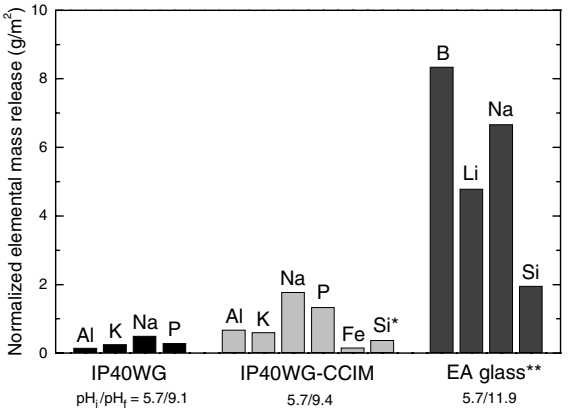

Fig. 4. Normalized elemental mass release (g/m^2) from iron phosphate and environmental assessment (EA) glasses after PCT in DIW at 90 °C for seven days. Elements for which the mass release is less than 0.01 g/m^2 are not shown. The initial (pH$_i$) and final (pH$_f$) pH of the leachate is given for each glass. * Arbitrary Si from the sacrificial conductive silicon carbide. ** DOE requirement for HLW [21,22].

IP40WG-CCIM iron phosphate glasses was ~25 and ~5 times, respectively, smaller than that of the EA glass in DIW at 90 °C. It should be noted that the increase in the pH of the leachate for the IPGs was much smaller (from the initial value of 5.8 to a maximum of 6.9) than the increase for the EA glass (from 5.8 to 8.9). This small change in pH for the leachate from iron phosphate glasses has been noted previously [18–20], which is evidence of a buffering action for phosphate glasses and which is believed to be absent for borosilicate glasses.

The normalized elemental mass release (r_i) from the PCT results for the iron phosphate (IP40WG and IP40WG-CCIM) and EA glasses is given in Fig. 4. The PCT protocol was designed specifically for borosilicate glasses and the established representative elements for PCT release for BS glasses are B, Li, and Na. There is no established PCT specification for phosphate glasses and both IP40WG and IP40WG-CCIM glasses do not contain either B (very little, 0.1 wt% B_2O_3, for IP40WG) or Li. Therefore, the normalized elemental mass release, r_{Na}, for sodium which is the only common element present in both the iron phosphate and borosilicate glasses is used here to compare the chemical durability from PCT for these glasses. The values of r_i for a few other elements such as Al, K, P, and Fe have also been included in Fig. 4.

The r_{Na} released from IP40WG and IP40WG-CCIM was only 0.5 and 1.8 g/m^2, respectively. These values of r_{Na} were ~13 and ~4 times smaller than the current DOE specification (r_{Na} = 6.67 [21,22]) for the EA borosilicate glass. The chemical durability of the IP40WG-CCIM was not as good as that of the conventionally melted IP40WG, but was still considerably better than that of the EA glass. The pH of the DIW used for the PCT increased more for the borosilicate glass (by a factor of 2.09) compared to that for the iron phosphate glasses (by a factor of 1.60–1.65), see Fig. 4. This smaller change in pH for iron phosphate glasses is due to their larger buffering action, compared to silicate glasses, in the solution.

The surface morphology of the as-made IP40WG and IP40WG-CCIM glass particles as viewed by SEM is shown in Fig. 5(a) and (c), respectively, and that of the glass particles after the 7 day PCT is shown in Fig. 5(b) and (d) respectively. The sharp corners and edges initially present in the as-made particles, Fig. 5(a) or (c) were retained in the particles after PCT, Fig. 5(b) or (d). Also, there was no noticeable corrosion of the glass particles after the PCT. The retention of the sharpness at the corners and edges, and absence of any detectable corrosion layer on the surface of the post-PCT glass particles provide another evidence for the excellent chemical durability of the IP40WG and IP40WG-CCIM wasteforms.

Fig. 6 shows the appearance of the cross-section (a, c) and external surface (b, d) of the IP40WG and IP40WG-CCIM glasses, respectively, after the 7-day VHT at 200 °C. There was hardly any detectable corrosion on the surface of the IP40WG glass (Fig. 6(a)). The polishing lines were still observable, and only a few corrosion products, heterogeneously distributed on the surface, were visible (Fig. 6(b)). These small particles (corrosion products) were identified by XRD to be $Na_3Al(PO_4)_2 \cdot 1.5H_2O$ (Fig. 7(a)).

For the IP40WG-CCIM sample, a thin (~200 μm) corrosion layer was seen on the surface (Fig. 6(c)) and the alteration products are seen in Fig. 6(d). The VHT corrosion products from the IP40WG-CCIM sample

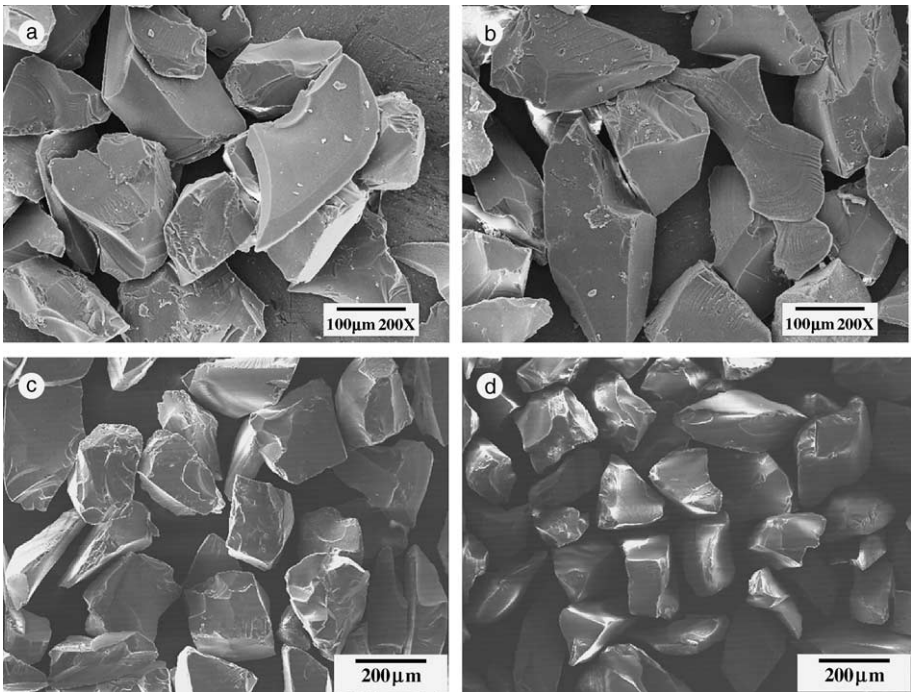

Fig. 5. (a) SEM photomicrographs of as-made IP40WG glass particles and (b) after immersion in deionized water at 90 °C for seven days (PCT). (c) As-made IP40WG-CCIM glass particles and (d) after PCT.

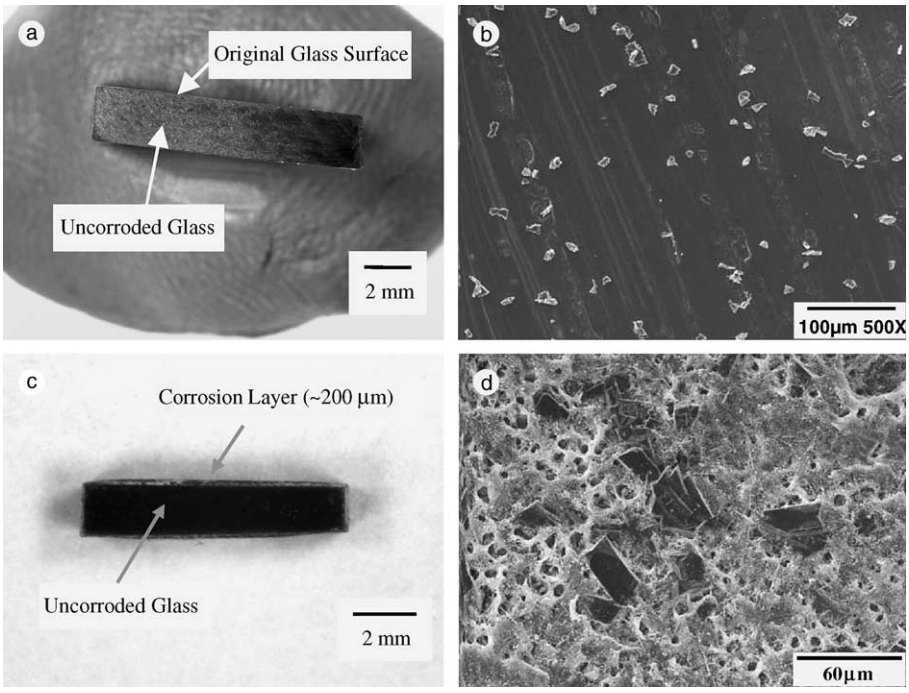

Fig. 6. Optical photo- (a), (c) and SEM photomicrographs (b), (d) of the IP40WG and IP40WG-CCIM specimens after the VHT (200 °C for seven days). (a) Cross-sectional view of IP40WG: no corroded layer was detectable on the surface; (b) external surface of IP40WG: polishing features still remained and only a few visible corrosion products were heterogeneously distributed on the surface; (c) cross-sectional view of IP40WG-CCIM: very thin corrosion layer was seen on the surface; (d) external surface of IP40WG-CCIM.

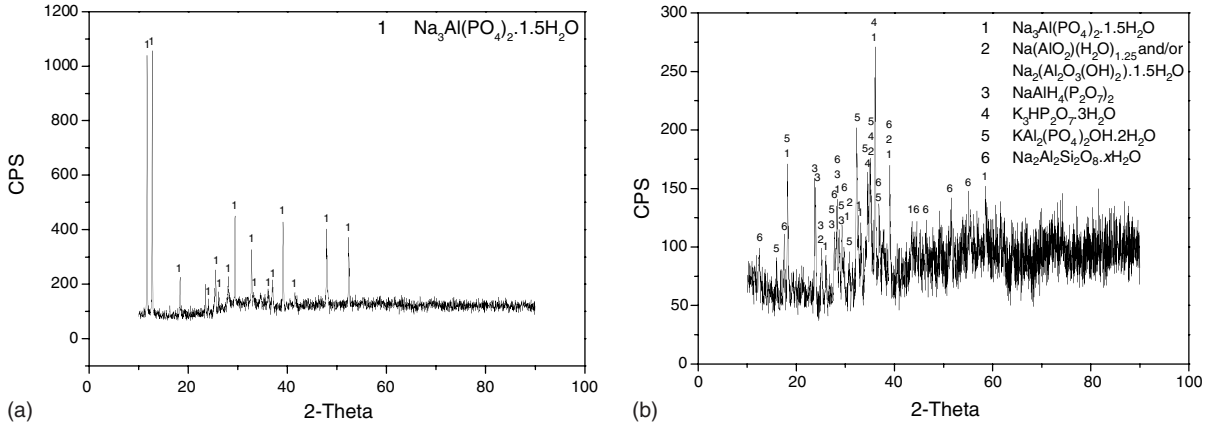

Fig. 7. XRD (CuK_α radiation) patterns for the corrosion products from IP40WG (a) and IP40WG-CCIM (b) samples after VHT at 200 °C for 7 days.

consisted of many phases such as $Na_3Al(PO_4)_2 \cdot 1.5H_2O$, $Na(AlO_2)(H_2O)_{1.25}$, $NaAlH_4(P_2O_7)_2$, $K_3HP_2O_7 \cdot 3H_2O$, and $Na_2Al_2Si_2O_8 \cdot xH_2O$, see XRD pattern in Fig. 7(b).

The corrosion rate for the IP40WG and IP40WG-CCIM glasses from the VHT was only <0.2 and 40 g/m^2/day, respectively (see Table 5). Currently, there is no DOE specification for VHT for HLW, but these values can be compared to the VHT specification (50 g/m^2/day [22,23]) for low activity waste (LAW), indicating that the IP40WG and IP40WG-CCIM glasses had an outstanding chemical resistance to the humid conditions at 200 °C for seven days.

The chemical durability measured by three independent techniques (D_R, PCT, and VHT) for the IP40WG and IP40WG-CCIM wasteforms were not only in excellent agreement with each other, but also showed that both wasteforms meet all current DOE requirements for chemical durability. The slightly poorer chemical durability of the IP40WG-CCIM glass, compared to that of the conventionally melted IP40WG glass, was possibly due to the presence of significant amounts of Fe(II), and the different raw materials and procedures used to prepare this glass.

Table 5
VHT corrosion rates (g/m^2/day) for iron phosphate glasses (IP40WG and IP40WG-CCIM) tested at 200 °C for 7 days

Wasteform	Corrosion rate (g/m^2/day)
IP40WG	<0.2
IP40WG-CCIM	40
DOE Limit[a]	50 [22,23]

[a] DOE specification for low activity waste (LAW) is given for comparison because, currently, there is no DOE specification for VHT for high level waste (HLW) [22,23].

3.6. Structure

The Mössbauer spectra of the IP40WG and IP40WG-CCIM glasses measured at room temperature are shown in Fig. 8. The speciation of the irons and hyperfine parameters extracted from the Mössbauer spectra are given in Table 6. The isomer shift for Fe(II) and Fe(III) ranges from 1.11 to 1.19 mm/s and from 0.40 to 0.42 mm/s, respectively, while the quadrupole splitting ranges from 2.08 to 2.11 mm/s and from 0.76 to 0.84 mm/s, respectively. These values are in accordance with the previously reported values [8,24] in the iron phosphate glasses. The values for the isomer shift correspond to octahedral or distorted octahedral coordination for both Fe(II) and Fe(III) ions in these glasses.

The IP40WG glass contains 11% Fe(II) while the IP40WG-CCIM glass contains 56% Fe(II). More of the Fe(III) ions in the starting batch of IP40WG-CCIM were reduced to Fe(II) ions during melting in the CCIM than were reduced in the IP40WG when conventionally melted in an electric furnace. The more reducing conditions for the IP40WG-CCIM melt could be due to the presence of carbonates and silicon carbide in the starting batch and/or to a higher melt temperature in the CCIM. The significantly higher amount of Fe(II) in the IP40WG-CCIM glass is a likely reason for the higher D_R values, PCT release, and VHT corrosion compared to those of the conventionally melted IP40WG glass.

The IR spectra for the IP40WG and IP40WG-CCIM glasses are shown in Fig. 9. The bands at 1160–1170 cm^{-1} are attributed to the symmetric vibration of phosphorus and non-bridging oxygen in metaphosphate (Q^2) groups $(PO_3)^{-1}$ [25,26]. The bands at 1080–1100 and 740 cm^{-1} are assigned to the symmetric stretching modes of non-bridging oxygen and bridging (P–O–P) oxygen, respectively, in Q^1 pyro structure $(P_2O_7)^{-4}$

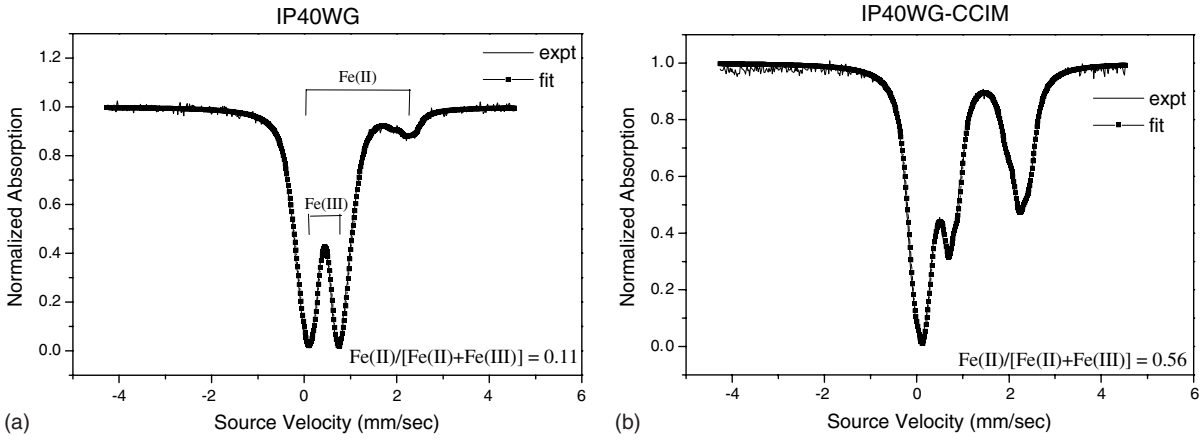

Fig. 8. Mössbauer spectra at room temperature for (a) IP40WG and (b) IP40WG-CCIM wasteforms.

Table 6
Room temperature Mössbauer hyperfine parameters (IS: isomer shift in mm/s, QS: quadrupole splitting in mm/s) and fraction of Fe(II) for IP40WG and IP40WG-CCIM wasteforms

Wasteform	IS		QS		% Fe(II) fraction[a]
	Fe(II)	Fe(III)	Fe(II)	Fe(III)	
IP40WG	1.11	0.42	2.08	0.84	11
IP40WG-CCIM	1.19	0.40	2.11	0.76	56

The estimated error in IS and QS is ±0.03 mm/s.
[a] Fe(II)/[Fe(II) + Fe(III)] as calculated from Mössbauer spectra.

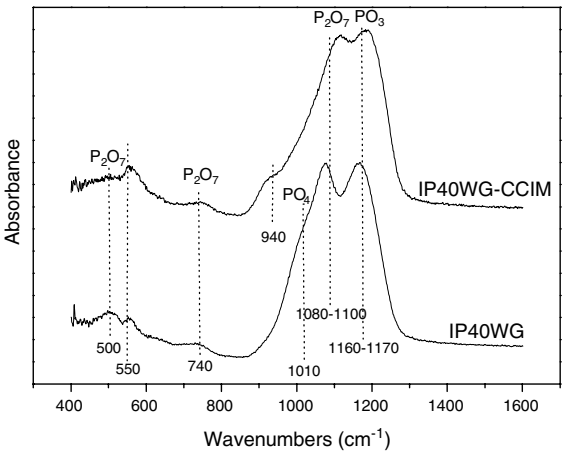

Fig. 9. The IR spectra of IP40WG and IP40WG-CCIM glasses.

[25,26]. The shoulder at 1010 cm^{-1} in the spectra for the IP40WG glass suggests the presence of isolated $(PO_4)^{-3}$ orthophosphate groups (Q^0), implying that the IP40WG glass contains bands characteristic of all three phosphate groups in the glass network, while the Q^0 groups are absent in the IP40WG-CCIM glass.

A shoulder at 940 cm^{-1} in the spectra for the IP40WG-CCIM glass may be associated with the presence of SiO_2 in this glass. The assignment of the bands at 550 cm^{-1} is uncertain, but the bands at 500 cm^{-1} have been assigned to the motion of Fe–O polyhedron and $(P_2O_7)^{-4}$ group in Q^1 groups [27,28]. The absence of isolated PO_4 groups in the IP40WG-CCIM glass may be due to the presence of significant amounts of Fe(II) in the glass. The higher amount of Fe(II) (less oxygen in the glass network) may increase the number of PO_3 groups (Fig. 9) in the IP40WG-CCIM glass. The larger amounts of PO_3 groups as well as the presence of SiO_2 in the glass network might lower the chemical durability of the IP40WG-CCIM wasteform. However, previous studies [10,11] have shown that the structure of the baseline iron phosphate glass $43Fe_2O_3 \cdot 57P_2O_5$, wt% did not change with increasing fraction of Fe(II). It has been reported [8,29,30] that P_2O_7 and PO_4 groups are more chemically durable than metaphosphate groups which contain more P–O–P bonds that are easily hydrolyzed.

The Raman spectra of the IP40WG and IP40WG-CCIM glasses in Fig. 10 show the same structural groups as seen in the IR spectra of these glasses. The bands at 1160 and 620 cm^{-1} are due to the symmetric stretching vibrations of phosphorus and non-bridging

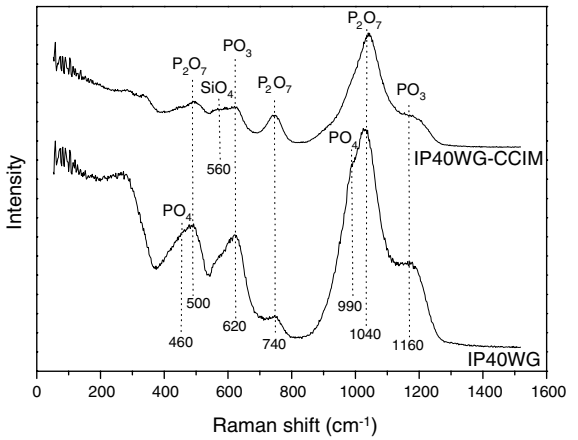

Fig. 10. Raman spectra of IP40WG and IP40WG-CCIM glasses.

oxygen and bridging oxygen, respectively, in Q^2 groups [16]. The most prominent bands at 1040 and 740 cm^{-1} are attributed to the stretching mode of non-bridging oxygen and P–O–P stretching of the bridging oxygen in pyrophosphate groups, P_2O_7, respectively [16]. The shoulders at 990 and 460 cm^{-1} in the IP40WG glass suggest the presence of isolated Q^0 groups, while the Q^0 groups are absent in the IP40WG-CCIM glass, which agrees with the IR spectra.

A weak peak at 560 cm^{-1} is probably associated with the SiO_2 in IP40WG-CCIM glass. This band could be related to the bridging oxygen in SiO_4 (Q^4) groups. The bands at 500 cm^{-1} are assigned [16] to the vibrations of Fe–O and P_2O_7 groups which are characteristic for a network structure dominated by pyrophosphate groups. Low frequency bands are due to bending modes of chains in the glass.

4. Conclusions

The present investigation has demonstrated several advantages for vitrifying the SBW stored at INEEL in iron phosphate glass wasteforms (IP40WG and IP40WG-CCIM), if vitrification of this waste is reconsidered in the future. Among these advantages is a high waste loading (40 wt%) of the simulated SBW and the successful melting in a CCIM, as an alternative to conventional melting in an electric furnace. The successful melting of small amounts (~1 kg) of the IP40WG glass in the CCIM is highly encouraging since any potential corrosion problems involving glass contact refractories and metal electrode materials needed for joule heated melting are avoided. Based on the present results, CCIM appears to be a viable technique for melting iron phosphate glasses on a large-scale. This viability was also suggested by the higher electrical conductivity measured for the IPG melts near their melting temperature range.

The chemical durability of the IP40WG and IP40WG-CCIM vitrified wasteforms meets all the current DOE requirements. The durability of the IP40WG-CCIM glass was slightly poorer compared to that of the IP40WG glass probably because of the larger amount of Fe(II) in the glass and the relatively large number of P–O–P bonds in the glass structure. The more reducing conditions which apparently existed for the IP40WG-CCIM glass were likely due to the carbonates and SiC in the batch and to a higher melting temperature in the CCIM. Based on the present data from a single experiment in the CCIM, it is anticipated that additional CCIM tests should produce iron phosphate glasses with improved chemical durability.

Iron phosphate glasses containing 40 wt% SBW can be melted as low as 950–1000 °C without sulfate segregation. Because these melts have a high fluidity (low viscosity at the melting temperature) and become rapidly homogeneous, melting times can be as short as a few hours (<6 h) compared to the ~48 h needed for borosilicate glasses. The high waste loading, low melting temperature, rapid furnace throughput (short melting times), and the potential for melting iron phosphate glasses in a CCIM should significantly reduce the cost of vitrifying the Sodium Bearing Waste stored at INEEL.

Acknowledgements

This work is being performed under the Environmental Management Science Program (EMSP) of the US Department of Energy (DOE). The authors would like to thank DOE for supporting this research under contract FG07-96ER45618.

References

[1] S.L. Lambert, D.S. Kim, Pacific Northwest National Laboratory Report, PNNL #WHC-SP-1143, 1994.
[2] J.M. Perez Jr., D.F. Bickford, D.E. Day, D.S. Kim, S.L. Lambert, S.L. Marra, D.K. Peeler, D.M. Strachan, M.B. Triplett, J.D. Vienna, R.S. Wittman, Pacific Northwest National Laboratory Report, PNNL-13582, 2001.
[3] D. Gombert, Idaho National Engineering and Environmental Laboratory Report, INEEL/EXT-01-01213, 2001.
[4] D.R. Lide (Ed.), CRC Handbook of Chemistry and Physics, 82nd ed., CRC, 2001/2002.
[5] D.E. Day, Z. Wu, C.S. Ray, P. Hrma, J. Non-Cryst. Solids 241 (1998) 1.
[6] American Society for Testing and Materials (ASTM), Standard Test Methods for Determining Chemical Durability of Nuclear, Hazardous, and Mixed Waste Glasses: The Product Consistency Test (PCT), C 1285-97, 1998.

[7] A. Jiricka, Pacific Northwest National Laboratory Technical Procedure, GDL-VHT, Rev. 1, 2000.
[8] G.K. Marasinghe, M. Karabulut, C.S. Ray, D.E. Day, M.G. Shumsky, W.B. Yelon, C.H. Booth, P.G. Allen, D.K. Shuh, J. Non-Cryst. Solids 222 (1997) 144.
[9] G.K. Sullivan, M.H. Langowski, P. Hrma, Ceram. Trans. 61 (1995) 187.
[10] C.S. Ray, X. Fang, M. Karabulut, G.K. Marasinghe, D.E. Day, J. Non-Cryst. Solids 249 (1999) 1.
[11] X. Fang, C.S. Ray, A. Moguš-Milanković, D.E. Day, J. Non-Cryst. Solids 283 (2001) 162.
[12] R. Doremus, Glass Science, Wiley, 1994.
[13] J.D. Vienna, Pacific Northwest National Laboratory, 2002, Personal communication.
[14] D.E. Day, J. Non-Cryst. Solids 21 (1976) 343.
[15] L. Murawski, J. Mater. Sci. 17 (1982) 2155.
[16] A. Moguš-Milanković, B. Šantić, D.E. Day, C.S. Ray, J. Non-Cryst. Solids 283 (2001) 119.
[17] A. Moguš-Milanković, A. Šantić, A. Gajović, D.E. Day, J. Non-Cryst. Solids 296 (2001) 57.
[18] X. Yu, D.E. Day, Proc. 17th Int. Congress Glass 2 (1995) 45.
[19] G.K. Marasinghe, M. Karabulut, C.S. Ray, D.E. Day, C.H. Booth, P.G. Allen, D.K. Shuh, Ceram. Trans. 87 (1998) 261.
[20] M.G. Mesko, D.E. Day, B.C. Bunker, Immobilization of high-level radioactive sludges in iron phosphate glass in Science and Technology for Disposal of Radioactive Tank Wastes, Plenum Press, New York, 1998.
[21] C.M. Jantzen, N.E. Bibler, D.C. Beam, C.L. Crawford, M.A. Pickett, Westinghouse Savannah River Company Report, WSRC-TR-92-346, Rev. 1, 1993.
[22] US DOE, Design, Construction, and Commissioning of the Hanford Tank Waste Treatment and Immobilization Plant, US Department of Energy (DOE), Contract no. DE-AC27-01RV14136, DOE Office of River Protection, Richland, WA, Contract with Bechtel National, Inc., San Francisco, CA, 2001.
[23] A. Jirica, J.D. Vienna, P. Hrma, D.M. Strachan, J. Non-Cryst. Solids 292 (2001) 25.
[24] M. Karabulut, G.K. Marasinghe, C.S. Ray, D.E. Day, G.D. Waddill, C.H. Booth, P.G. Allen, J.J. Bucher, D.L. Caulder, D.K. Shuh, J. Non-Cryst. Solids 306 (2002) 182.
[25] B. Samuneva, P. Tzvetkova, I. Gugov, V. Dimitrov, J. Mater. Sci. Lett. 15 (1996) 2180.
[26] A.M. Efimov, J. Non-Cryst. Solids 209 (1997) 209.
[27] G. Wang, Y. Wang, B. Jin, SPIE 2287 (1994) 214.
[28] X. Fang, C.S. Ray, G.K. Marasinghe, D.E. Day, J. Non-Cryst. Solids 263&264 (2000) 293.
[29] X. Yu, D.E. Day, G.J. Long, R.K. Brow, J. Non-Cryst. Solids 215 (1997) 21.
[30] G.K. Marasinghe, M. Karabulut, C.S. Ray, D.E. Day, D.K. Shuh, P.G. Allen, M.L. Saboungi, M. Grimsditch, D. Haeffner, J. Non-Cryst. Solids 263&264 (2000) 146.